Semnan University

Mechanics of Advanced Composite Structures

Journal homepage: https://macs.semnan.ac.ir/

ISSN: 2423-7043

Research Article

Vibration Analysis of FGM Annular Plate with Linearly Varying Thickness for Several Boundary Conditions

Sumit Kumar Sharma, Neha Ahlawat *

Department of Mathematics, Jaypee Institute of Information Technology, Noida-201303, India

ARTICLE INFO

Article history:

Received: 2025-03-05
Revised: 2025-09-02
Accepted: 2025-11-25

Keywords:

FGM;
Variable thickness;
Annular plate;
Axisymmetric vibration;
DTM.

ABSTRACT

The present article depicts the influence of linear thickness variation on the free axisymmetric vibration of functionally graded material annular plates. For this, three different types of boundary conditions have been taken into consideration. An ordinary differential equation of fourth order has been formulated using classical plate theory and Hamilton's principle. The differential transform method has been developed for the numerical solution of such a differential equation along with three boundary conditions. The obtained numerical results are reported and then analyzed by varying the various parameters, like volume fraction index of plate materials, radius ratio, and taper parameter. The comparative study has also been made to validate the obtained numerical results as well as the technique. It has been observed that natural frequencies drop as the volume fraction index rises. The frequency parameter usually increases with a smaller radius ratio. A decrease in the natural frequency value has been seen when the plate thickness increases. Moreover, the 3-D mode shapes for all the plates are also presented.

1. Introduction

Several structural components are made in the form of annular plates, and these components have been widely used in static and dynamic systems. In many practical applications, for the requirement of different designs, different materials for the top and bottom surfaces of the plate are being used. For this situation, FGM is the best component, which is the advancement of the composite materials having continuous and smooth variation of mechanical properties defined in one or more directions, which is formed by using a combination of different types of metals and ceramics. FGM was developed in 1984 by Japanese researchers for their aerospace project.

Due to various advantages of FGM over conventional composite materials, the plates made of these materials are widely used not only in aerospace engineering but also in various other engineering applications. The free vibration of multi-directional FG annular and circular plates has been studied by Kermani et al. [1] using DQM. Asemi et al. [2] have analysed three-dimensional biaxial buckling of an FG annular sector plate, which is fully or partially supported on a Winkler

* **Corresponding author.**
E-mail address: *ahlawatneha@gmail.com* & *neha.ahlawat@jiit.ac.in*

Cite this article as:
Sharma, S. K. and Ahlawat, N., 2026. Vibration Analysis of FGM Annular Plate with Linearly Varying Thickness for Several Boundary Conditions. *Mechanics of Advanced Composite Structures*, 13(2), pp. 475-494.
https://doi.org/10.22075/MACS.2025.37061.1812

elastic foundation. Later, Asemi et al. [3] studied the shear buckling of FGM annular sector plates. Wang et al. [4] developed a method for the unified solution of the vibration of FGM sector, annular, and circular plates with general boundary conditions. The effect of hydrostatic in-plane force on the radially symmetric vibrations of two-directional functionally graded circular plates has been presented by Lal and Ahlawat [5]. The analysis of the vibration of FGM annular plates, which are elastically supported, has been done by Żur [6] via the Quasi-Green's function method. Civalek et al. [7] have analysed the vibration of a carbon nanotube reinforced composite annular sector plate by using the discrete singular convolution method. Zhang et al. [8] presented a vast review of the work that was done on stability analysis, buckling, and free vibration of FGM plates. The finite annular prism method has been used by Wu and Yu [9] to analyse the vibration of two-directional FGM plates. Tash and Neya [10] presented a solution for the bending of transversely isotropic thick rectangular plates with variable thickness. Eshraghi and Dag [11] analysed the forced vibration of FG circular and annular plates by using the domain-boundary element method. The analysis on the vibration of an FG annular plate having edge supports and resting on a Winkler foundation has been done by Hashemi et al. [12]. Javani et al. [13] (2021) presented thermally induced vibrations of an FGM annular sector plate using GDQM. Arefi et al. [14] have analysed the graphene nanoplatelets reinforced cylindrical shell subjected to thermo-mechanical loads based on shear deformation theory. The thermal post-buckling analysis of functionally graded annular sector plates exposed to uniform temperature rise has been presented by Shahsavari et al. [15] for the first time. The hygrothermal influence on the natural frequencies of functionally graded circular plates with piezo-magneto-electro-elastic layers sitting on a Pasternak elastic foundation has been studied by Kiarasi et al. [16]. Sobhani et al. [17] have analysed the vibrational behaviour of coupled hemispherical-conical-conical shells structures made of composite materials reinforced with nanofillers. Vasara et al. [18] have used DQM to analyse the vibration of FG annular and circular plates. Huang and Chung [19] presented an analytical solution based on three-dimensional elasticity for the vibrations of an FGM rectangular plate with two simply supported opposite faces. Shariati et al. [20] presented the vibrational characteristics of an annular FGM nano-plate using FSDT. Khatoonabadi et al. [21] have examined the shear buckling of a functionally graded porous annular sector plate reinforced with graphene nanoplatelets. Recently, Sharma and Ahlawat [22] have studied the axisymmetric vibration of FGM annular plates using DTM. Bridjesh et al. [23] have analysed the buckling of a two-directional porous FG beam using higher-order shear deformation theory.

Moreover, the plates with varying thickness gained a lot of popularity as these types of plates fulfil the practical requirements of the structural components more effectively. Such plates are highly preferred these days due to their affordability and lightness, especially in modern structures and aerospace technology. Lal and Sharma [24] used the Chebyshev collocation method to study the vibrations of non-homogeneous polar orthotropic annular plates with variable thickness. Alipour et al. [25] analysed the vibration of a two-directional FGM circular plate resting on an elastic foundation with varying thickness. Hosseini et al. [26] analysed the vibration of tapered FG circular and annular sectorial thin plates resting on a Pasternak elastic foundation. DTM has been used by Lal and Ahlawat [27] to study the vibration and buckling of an FGM circular plate with linear thickness resting on a Winkler foundation. Lal and Rani [28] studied the axisymmetric vibration of circular sandwich plates of linearly varying thickness using DQM. Gupta et al. [29] have analysed the effect of non-uniform thickness on the vibration of partially cracked isotropic and FGM micro-plates. The vibration of an FGM circular plate, which depends on temperature with nonlinear thickness, has been analysed by Lal and Saini [30]. Ahlawat and Lal [31] have studied the radially symmetric vibration of an FGM circular plate with linearly varying thickness resting on a Winkler foundation subjected to a uniform tensile in-plane force. Using the hyperbolic shear deformation theory, Talebitouti et al. [32] determined the FG plate's acoustic transmission. Lal and Saini [33] have analysed the vibration of an FG circular plate of variable thickness under a thermal environment by GDQM. The vibration of a tapered circular poroelastic plate has been studied by Jalali and Heshmati [34] by using the pseudo-spectral method. Tran and Thai [35] presented an isogeometric analysis to study the dynamic behaviour of multi-directional FG plates with variable thickness. The study of vibration of multidirectional FG sector, elliptical, and circular plates with variable thickness has been presented by Zhong et al. [36]. Hashemi et al. [37] analysed the vibration of an FG rectangular non-linear plate using FSDT. Kumar et al. [38] have used Galerkin-Vlasov's method to study of vibration of an FGM plate with linearly varying thickness. Minh et al. [39] studied the vibration of a cracked FGM plate resting on an elastic foundation along with thickness variation. Zarastvand et al. [40] provide a review study that was created to

compile, categorize, and arrange all of the earlier studies on the sound-isolating properties of plate structures. A systematic overview of all the previous studies on sound transmission across multilayered plate constructions is presented by Zarastvand et al. [41]. In their investigation of the behaviour of sound propagation in three-dimensional (3D) sandwich panels, Ghafouri et al. [42] highlight the function of 3D Re-Entrant Auxetic Cellular Structures (RACSs) in the panel core. Kumar et al. [43] have analysed the vibration of a tapered porous FGM plate resting on an elastic foundation. Saini et al. [44] have analysed the effect of temperature variation on FGM rings with linearly varying thickness. Hadji et al. [45] analysed the buckling and vibration of multi-directional functionally graded sandwich plates subjected to various boundary conditions. Islam and Kedar [46] investigated the buckling behavior of a thin rectangular FGM plate with variable thickness under hygrothermal loads. The effect of non-linear thickness variation on radially symmetric vibration of bi-directional FGM circular plates resting on Winkler's foundation has been investigated by Ahlawat and Saini [47]. Recently, the free vibration properties of rotating pre-twisted porous sigmoid functionally graded material plates with bi-directional thickness variation were examined by Mandal et al. [48]. The vibration properties of composite shells with a cylindrical-hemispherical geometry made of functionally graded porous materials in different thicknesses have been studied by Jafari and Shaterzadeh [49].

Keeping the above work in view, the effect of linearly varying thickness on the axisymmetric vibrations of annular FGM plates has not been collectively explored yet. Hence, in the present work, a semi-analytical technique called DTM [50] has been used to analyse this effect, in which the obtained ordinary differential equation of fourth order is reduced to frequency equations that have been derived for the three sets of boundary conditions, namely clamped-clamped, clamped-simply supported, and clamped-free. In this method, recurrence relations are obtained from the governing differential equation and the boundary conditions. These relations are then solved using MATLAB, and the values of the frequency parameter are obtained by varying the values of different parameters. The comparative study has also been made to verify the obtained numerical results as well as the technique.

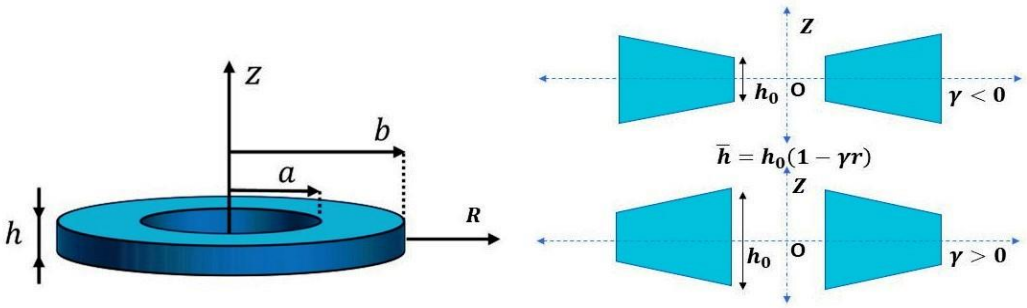

Fig. 1. Thickness variation of the annular FGM plate

2. Mathematical Formulation

The annular FGM plate (Fig. 1) has been taken with outer and inner radius as b and a, respectively. The plate thickness is assumed as h and the material density as d. A cylindrical polar coordinate system (R, θ, z) has been taken as a reference for the present plate, where $z = 0$ is the middle plane, $R = 0$ is the axis, $z = h/2$ is the upper surface and $z = -h/2$ is the lower surface of the plate.

The governing fourth-order differential equation of motion, which represents the axisymmetric vibration of the FGM annular plate (Fig. 1), is given by [51]:

$$D\,x_{,RRRR} + \frac{2}{R}\left[RD_{,R} + D\right]x_{,RRR} + \frac{1}{R^2}\left[R^2 D_{,RR} + R(2+\upsilon)D_{,R} - D\right]x_{,RR} + \frac{1}{R^3}\left[R^2\upsilon D_{,RR} - RD_{,R} + D\right]x_{,R} + hd\,x_{,tt} = 0 \quad (1)$$

where D is the flexural rigidity and x is the transverse deflection.

The deflection x can be expressed for the harmonic vibrations as [22]:

$$x(t, R) = X(R)e^{i\omega t} \quad (2)$$

here, ω represents the frequency in radians.

From Eqs (1) and (2), we get

$$D\frac{d^4X}{dR^4}+\frac{2}{R}\left[RD_{,R}+D\right]\frac{d^3X}{dR^3}+$$
$$\frac{1}{R^2}\left[R^2D_{,RR}+R(\upsilon+2)D_{,R}-D\right]\frac{d^2X}{dR^2}+ \quad (3)$$
$$\frac{1}{R^3}\left[R^2\upsilon D_{,RR}-RD_{,R}+D\right]\frac{dX}{dR}-dhX\omega^2=0$$

We consider here that the lower surface of the FGM plate is made from metal and the upper surface is made from ceramic. The mechanical properties, i.e., density $d(z)$ and Young's modulus $Y(z)$ which are varying in z-direction, have been written as [52]:

$$Y(z)=\left[(Y_2-Y_1)V_2(z)+Y_1\right] \quad (4)$$

$$d(z)=\left[(d_2-d_1)V_2(z)+d_1\right] \quad (5)$$

where Y_1, Y_2 represents the Young's modulus and d_1, d_2 represents the density of metal and ceramic constituents, respectively.

Now, the volume fraction of ceramic $V_2(z)$ has been taken as

$$V_2(z)=\left(\frac{z}{h}+\frac{1}{2}\right)^g \quad (6)$$

where g represents the VFI of the ceramic.

Here, taking the mathematical expressions for D and d as given below [27]

$$D=\frac{1}{1-\upsilon^2}\int_{-h/2}^{h/2}Y(z)z^2dz \quad (7)$$

$$d=\frac{1}{h}\int_{-h/2}^{h/2}d(z)dz \quad (8)$$

Combining the Eqs. (4-6) with the Eqs. (7-8), we get,

$$D=\frac{h^3Y_2S}{12\left(1-\upsilon^2\right)} \quad (9)$$

$$d=\frac{d_1g+d_2}{g+1} \quad (10)$$

where

$$S=\left[\frac{Y_1}{Y_2}+3\left(1-\frac{Y_1}{Y_2}\right)\frac{g^2+g+2}{(g+1)(g+2)(g+3)}\right]$$

In order to make the variables non-dimensional, we are using $\frac{R}{b}=r$, $\frac{X}{b}=p$, $\frac{h}{b}=\bar{h}$ in Eq. (3), we get

$$D\frac{d^4p}{dr^4}+\frac{2}{r}\left[rD_{,r}+D\right]\frac{d^3p}{dr^3}+$$
$$\frac{1}{r^2}\left[r^2D_{,rr}+r(\upsilon+2)D_{,r}-D\right]\frac{d^2p}{dr^2}+ \quad (11)$$
$$\frac{1}{r^3}\left[r^2\upsilon D_{,rr}-rD_{,r}+D\right]\frac{dp}{dr}=d\bar{h}\omega^2b^5p$$

Using $\bar{h}=h_0(1-\gamma r)$ for linear variation in the thickness, where h_0 is the dimensionless thickness at the inner boundary of the plate and γ is the taper parameter of the plate.

Substituting the values obtained in Eqs. (9-10) into Eq. (11), we get

$$\frac{d^4p}{dr^4}+2\left[-\frac{3\gamma}{(1-r\gamma)}+\frac{1}{r}\right]\frac{d^3p}{dr^3}+$$
$$\left[\frac{6\gamma^2}{(1-\gamma r)^2}-\frac{3\gamma(\upsilon+2)}{r(1-r\gamma)}-\frac{1}{r^2}\right]\frac{d^2p}{dr^2} \quad (12)$$
$$+\left[\frac{6\gamma^2\upsilon}{r(1-r\gamma)^2}+\frac{3\gamma}{r^2(1-r\gamma)}+\frac{1}{r^3}\right]\frac{dp}{dr}$$
$$=\frac{\Omega^2A}{S(1-r\gamma)^2}p$$

where

$$\Omega^2=\frac{d_2h_0b^2}{D^*}\omega^2, \qquad D^*=\frac{Y_2h_0^{\,3}}{12(1-\upsilon^2)},$$
$$S=\left[\frac{Y_1}{Y_2}+3\left(1-\frac{Y_1}{Y_2}\right)\frac{g^2+g+2}{(g+1)(g+2)(g+2)}\right],$$
$$A=\frac{d_1g+d_2}{d_2(g+1)}$$

Taking the centre at $r_0=b$, the power series expressions for different terms present in Eq. (12) are as follows [53]:

$$\frac{1}{r}=\sum_{i=0}^{N}-\left(-\frac{1}{b}\right)^{1+i}(r-b)^{i},$$

$$\frac{1}{r^{2}}=\sum_{i=0}^{N}(1+i)\left(-\frac{1}{b}\right)^{2+i}(r-b)^{i},$$

$$\frac{1}{r^{3}}=\sum_{i=0}^{N}-\frac{(2+i)(1+i)}{2}\left(-\frac{1}{b}\right)^{3+i}(r-b)^{i},$$

$$\frac{1}{1-r\gamma}=\sum_{i=0}^{N}r^{i}\gamma^{i},$$

$$\frac{1}{(1-r\gamma)^{2}}=\sum_{i=0}^{N}(1+i)r^{i}\gamma^{i},$$

$$\frac{1}{r(1-\gamma r)}=\sum_{i=0}^{N}r^{i-1}\gamma^{i},$$

$$\frac{1}{r^{2}(1-\gamma r)}=\sum_{i=0}^{N}r^{i-2}\gamma^{i},$$

$$\frac{1}{r(1-r\gamma)^{2}}=\sum_{i=0}^{N}(1+i)r^{i-1}\gamma^{i}$$

From Eq. (12), we have

$$\frac{d^{4}p}{dr^{4}}+$$

$$2\left\{-\sum_{i=0}^{N}\left(-\frac{1}{b}\right)^{1+i}(r-b)^{i}-3\gamma\sum_{i=0}^{N}r^{i}\gamma^{i}\right\}\frac{d^{3}p}{dr^{3}}$$

$$+\left\{\begin{array}{l}-\sum_{i=0}^{N}(1+i)\left(-\frac{1}{b}\right)^{2+i}(r-b)^{i}\\-3\gamma(\upsilon+2)\sum_{i=0}^{N}r^{i-1}\gamma^{i}+\\6\gamma^{2}\sum_{i=0}^{N}(1+i)r^{i}\gamma^{i}\end{array}\right\}\frac{d^{2}p}{dr^{2}}$$

$$+\left\{\begin{array}{l}-\sum_{i=0}^{N}\frac{(2+i)(1+i)}{2}\left(-\frac{1}{b}\right)^{3+i}(r-b)^{i}\\+3\gamma\sum_{i=0}^{N}\gamma^{i}r^{i-2}+6\upsilon\gamma^{2}\sum_{i=0}^{N}(1+i)\gamma^{i}r^{i-1}\end{array}\right\}\frac{dp}{dr}$$

$$=\frac{\Omega^{2}A}{S}\left\{\sum_{i=0}^{N}(1+i)r^{i}\gamma^{i}\right\}p \tag{13}$$

The accurate solution of Eq. (13) is not possible as it is a differential equation with variable coefficients; therefore, we are using DTM to obtain the numerical solution for suitable boundary conditions.

3. Boundary Conditions

We consider three types of boundary conditions on the plate as follows:

3.1. Clamped-Clamped: i.e., clamped at inner and outer boundaries

$$\begin{cases}p(a)=0, & \frac{dp}{dr}\big|_{r=a}=0\\ p(b)=0, & \frac{dp}{dr}\big|_{r=b}=0\end{cases} \tag{14-17}$$

3.2. Clamped-Simply supported: i.e., inner boundary is clamped and outer boundary is simply supported

$$\begin{cases}p(a)=0, & \frac{dp}{dr}\big|_{r=a}=0\\ p(b)=0,\\ M_{r}\big|_{r=b}=\left\{-D\left[\frac{d^{2}p}{dr^{2}}+\frac{\upsilon}{r}\frac{dp}{dr}\right]\right\}_{r=b}=0\end{cases} \tag{18-21}$$

where M_r is representing the bending moment in the radial direction.

3.3. Clamped-Free: i.e., inner boundary is clamped and outer boundary is free

$$\begin{cases}p(a)=0, & \frac{dp}{dr}\big|_{r=a}=0\\ (\text{at } r=b)\\ \frac{d^{2}p}{dr^{2}}+\frac{\upsilon}{r}\frac{dp}{dr}=0,\\ \frac{d^{3}p}{dr^{3}}+\frac{1}{r}\frac{d^{2}p}{dr^{2}}-\frac{1}{r^{2}}\frac{dp}{dr}=0\end{cases} \tag{22-25}$$

4. Method of Solution

Following [Lal and Ahlawat (2015)], let $p(r)$ be a function which is analytic in the domain and in that domain $r=r_0$ is any point. Then the differential transformation of n^{th} derivative of $p(r)$ will be

$$P_{n}=\frac{1}{n!}\left[\frac{d^{n}p(r)}{dr^{n}}\right]\ \text{at}\ \ r=r_{0} \tag{26}$$

and $$p(r)=\sum_{n=0}^{\infty}(r-r_{0})^{n}P_{n} \tag{27}$$

where P_n represents the transformed function and $p(r)$ represents the original function.

Combining Eq. (26) and (27) for a finite value of m, we get,

$$p(r)=\sum_{n=0}^{m}\frac{(r-r_{0})^{n}}{n!}\left[\frac{d^{n}p(r)}{dr^{n}}\right] \tag{28}$$

$$\text{at}\ \ r=r_{0}$$

The convergence of the frequency parameter will decide the number of terms m.

Table 1. Basic transformation rules are given as:

Original functions	Transformed functions
$p(j) = g(j) \pm l(j)$	$P_n = G_n \pm L_n$
$p(j) = \lambda g(j)$	$P_n = \lambda G_n$
$p(j) = g(j)l(j)$	$P_n = \sum_{i=0}^{n} G_i L_{n-i}$
$p(j) = \frac{d^k g(j)}{dj^k}$	$P_n = \frac{(n+k)!}{n!} G_{n+k}$
$p(j) = j^k$	$P_n = \delta(n-k) = \begin{Bmatrix} 0 & n \neq k \\ 1 & n = k \end{Bmatrix}$

4.1. Transformation of the Differential Equation

Now, employing Table 1 on Eq. (13), we get

$$\frac{(n+4)!}{n!}P_{n+4} - \sum_{i=0}^{n}\begin{bmatrix} 2\left(-\frac{1}{b}\right)^{1+i}\frac{(n+3-i)!}{(n-i)!} + \\ 6\gamma^{1+i}\frac{(n+3-i)!}{(n-i)!} + \\ 3(2+\upsilon)\gamma^{1+i}\frac{(n+3-i)!}{(n-i)!} \\ -3\gamma^{1+i}\frac{(n+3-i)!}{(n+2-i)!} \end{bmatrix} P_{n+3-i}$$

$$-\sum_{i=0}^{n}\begin{bmatrix} (1+i)\left(-\frac{1}{b}\right)^{2+i}\frac{(n+2-i)!}{(n-i)!} \\ -6(1+i)\gamma^{2+i}\frac{(n+2-i)!}{(n-i)!} - \\ 6\upsilon(1+i)\gamma^{2+i}\frac{(n+2-i)!}{(n-i+1)!} \end{bmatrix} P_{n+2-i}$$

$$-\sum_{i=0}^{n}\left[\frac{(2+i)(1+i)}{2}\left(-\frac{1}{b}\right)^{3+i}\frac{(n+1-i)!}{(n-i)!}\right]P_{n+1-i} = \frac{\Omega^2 A}{S}\sum_{i=0}^{n}(1+i)\gamma^i P_{n-i} \tag{29}$$

Replacing n by $(n-4)$ in the above equation, the frequency equation is given by

$$P_n = \frac{(n-4)!}{n!}\begin{bmatrix} \sum_{i=0}^{n-4}\begin{bmatrix} 2\left(-\frac{1}{b}\right)^{1+i}\frac{(n-i-1)!}{(n-i-4)!} \\ +6\gamma^{1+i}\frac{(n-i-1)!}{(n-i-4)!} \\ +3(2+\upsilon)\gamma^{1+i}\frac{(n-i-1)!}{(n-i-4)!} \\ -3\gamma^{1+i}\frac{(n-i-1)!}{(n-i-2)!} \end{bmatrix} P_{n-1-i} \\ +\sum_{i=0}^{n-4}\begin{bmatrix} (1+i)\left(-\frac{1}{b}\right)^{2+i}\frac{(n-i-2)!}{(n-i-4)!} \\ -6(1+i)\gamma^{2+i}\frac{(n-i-2)!}{(n-i-4)!} \\ -6\upsilon(1+i)\gamma^{2+i}\frac{(n-i-2)!}{(n-i-3)!} \end{bmatrix} P_{n-2-i} \\ +\sum_{i=0}^{n-4}\left[\frac{(2+i)(1+i)}{2}\left(-\frac{1}{b}\right)^{3+i}\frac{(n-i-3)!}{(n-i-4)!}\right]P_{n-3-i} \\ +\frac{\Omega^2 A}{S}\sum_{i=0}^{n-4}(1+i)\gamma^i P_{n-4-i} \end{bmatrix} \tag{30}$$

where $n = 0, 1, 2, \ldots\ldots\ldots, m$

4.2. Transformation of Boundary Conditions

Now, employing Table 1 on the boundary conditions, we get

4.2.1. Clamped-Clamped:

The transformed forms of Eqs. (14-15) at $r = a$ are

$$\sum_{n=0}^{m}(a-b)^n P_n = 0, \quad \sum_{n=1}^{m} n(a-b)^{n-1} P_n = 0 \tag{31-32}$$

and that of the Eqs. (16-17) at $r = b$ are

$$P_0 = 0, \quad P_1 = 0 \tag{33-34}$$

4.2.2. Clamped-Simply supported:

The transformed forms of Eqs. (18-19) at $r = a$ are

$$\sum_{n=0}^{m}(a-b)^n P_n = 0, \quad \sum_{n=1}^{m} n(a-b)^{n-1} P_n = 0 \tag{35-36}$$

and that of the Eqs. (20-21) at $r = b$ are

$$P_0 = 0,$$
$$(m+2)(m+1)P_{m+2} = \upsilon\sum_{i=0}^{m+1}\left(-\frac{1}{b}\right)^{1+i}(m+1-i)P_{m+1-i} \quad (37\text{-}38)$$

4.2.3. Clamped-Free:

The transformed forms of Eqs. (22-23) at $r = a$ are

$$\sum_{n=0}^{m}(a-b)^n P_n = 0, \quad \sum_{n=1}^{m} n(a-b)^{n-1} P_n = 0 \quad (39\text{-}40)$$

and that of the Eqs. (24-25) at $r = b$ are

$$(m+2)(m+1)P_{m+2} = \upsilon\sum_{i=0}^{m+1}\left(-\frac{1}{b}\right)^{1+i}(m+1-i)P_{m+1-i},$$
$$(m+3)(m+2)(m+1)P_{m+3} = \sum_{i=0}^{m+2}\left(-\frac{1}{b}\right)^{1+i}(m+2-i)(m+1-i)P_{m+2-i} + \sum_{i=0}^{m+1}(1+i)\left(-\frac{1}{b}\right)^{2+i}(m+1-i)P_{m+1-i} \quad (41\text{-}42)$$

5. Frequency Equations

Now, using the Eqs. (31-34) into Eq. (30) and putting $n = 4$ for the non-negative subscripts of the *P*-terms, we get recurrence relations in terms of P_2 and P_3 which is a system of homogeneous equations as follows:

$$U_1P_2 + U_2P_3 = 0$$
$$U_3P_2 + U_4P_3 = 0 \quad (43)$$

where U_1, U_2, U_3, U_4 are m^{th} degree polynomials in Ω.

Representing Eq. (43) in matrix form as:

$$\begin{bmatrix} U_1 & U_2 \\ U_3 & U_4 \end{bmatrix}\begin{bmatrix} P_2 \\ P_3 \end{bmatrix} = \begin{bmatrix} 0 \\ 0 \end{bmatrix} \quad (44)$$

The value of the determinant must be zero for the non-zero solution, so we have

$$\begin{vmatrix} U_1 & U_2 \\ U_3 & U_4 \end{vmatrix} = 0 \quad (45)$$

Similarly, the frequency equations for the two other boundary conditions can be obtained.

6. Numerical Results and Discussion

The frequency equations obtained for the three boundary conditions are solved using a MATLAB program, and values of the frequency parameter are obtained. Only the first three roots, i.e., the first three modes of these frequency equations, are reported and analyzed by varying the values of all the parameters, i.e. taper parameter. γ, radius ratio ε and VFI g. Here, we have chosen alumina as a ceramic and aluminium as a metal constituent, and for these two, the values of the parameters are taken from [27] as given below:

For aluminium

density $d_1 = 2702\ Kg/m^3$

and Young's modulus $Y_1 = 70\ GPa$,

For alumina

density $d_2 = 3800\ Kg/m^3$

and Young's modulus $Y_2 = 380\ GPa$

Poisson's ratio $\nu = 0.3$,

Taper parameter $\gamma = 0, \pm 0.1, \pm 0.3$

radii ratio $\varepsilon = \frac{a}{b} = 0.1, 0.2, 0.3$

and VFI g = 0, 1, 2, 3, 4, 5.

In order to fix the value of m, a MATLAB program was made and run, taking different values of all the parameters for all three boundary conditions, taking the value of $m = 17, 18, 19, 20, \ldots$ The value of $m = 20$ has been fixed as the difference between two successive values of Ω is smaller than 5×10^{-5} for all three boundary conditions and all three modes (Table 3).

Table 2 is the comparison table of the values of the frequency parameter. Ω in which the results were compared with those obtained by Sharma et al. [54] and Soni and Rao [55] by using the Chebyshev collocation technique for an isotropic FGM annular plate. We observe that the present results are very close for all three boundary conditions and all three modes, which represent the adaptability of the present method.

The numerical results are presented in Tables 4-6 and Figs. 2-10. We observe that the values of the frequency parameter Ω are lowest for the clamped-free boundary condition and highest for the same set of values of the parameter for the clamped-clamped boundary condition.

In Fig. 2-10, the behaviour of the frequency parameter Ω with varying values of the taper parameter $\gamma = 0, \pm 0.1, \pm 0.3$, VFI g = 0,1,2,3,4,5 and radii ratio ε = 0.1, 0.2, 0.3 for all three boundary conditions, and all three modes have been presented. Figs. 2-4 show the effect of VFI g on the frequency parameter on the three plates. It can be depicted that the value of the frequency

parameter Ω keeps changing from higher to smaller as the behaviour of the plate varies from isotropic (fully ceramic) to composite (FGM), i.e., with the increment in the values of VFI g. We also observe that this rate of change in the frequency parameter is more prominent when VFI $g \leq 2$ in comparison to $g \geq 3$ for all three modes and for all the plates. The frequency parameter values of an isotropic plate are larger than those of the comparable FGM plate, i.e., the frequency parameter falls with increasing metal constituent contribution.

The graphs between radii ratio ε and frequency parameter Ω are represented in Figs. 5-7 for a different set of values of VFI g and taper parameter γ. As the radius ratio $\varepsilon\left(=\frac{a}{b}\right)$ is the ratio of the inner radius a and outer radius b of the annular plate, respectively, so the plate becomes lighter when the annulus area of the plate is reduced. Here we are fixing the outer radius and varying the inner radius of the plate. From the graphs, we can observe that the value of the frequency parameter Ω increases whenever the value of the radius ratio ε increases. Hence, for all three boundary conditions, the frequency parameter likewise increases or decreases in proportion to the change in the radius ratio, or the hole size of the annular plate.

The graphs of the frequency parameter Ω and the taper parameter γ for the different sets of values of VFI g and radius ratio ε for all three modes and for all the plates, have been shown in Figs. 8-10. These graphs depict that the frequency parameter Ω decreases with increasing values of the taper parameter γ from -0.3 to 0.3 for the different sets of values of VFI g and radius ratio ε. So, as the taper parameter's values rise, the frequency parameter also rises.

Figs. 11-13 show the three-dimensional view of the three modes of the vibrations for all three boundary conditions, taking $\varepsilon = 0.1$, $g = 3$ and $\gamma = 0.1$.

Table 2. Comparison of frequency parameter Ω for isotropic plate (i.e. g= 0) taking $\varepsilon = 0.3, \gamma = 0.5$

Boundary Conditions	Ref.	MODE		
		I	II	III
C-C	Present	29.7276	82.6289	162.695
	[54]	29.7276	82.6289	162.6951
	[55]	29.7128	82.9526	---
C-S	Present	21.2689	67.7557	141.144
	[54]	21.2689	67.7557	141.1443
	[55]	21.2590	68.0115	---
C-F	Present	5.7907	31.147	84.6509
	[54]	---	---	---
	[55]	5.7713	31.0899	---

Table 3. Convergence of frequency parameter Ω taking at $\epsilon = 0.3, g = 3, \gamma = 0.3$

Boundary Conditions	m	I mode	II mode	III mode
C-C	19	27.9681	77.5461	152.491
	20	27.9681	77.5461	152.49
	21	27.9681	77.5461	152.49
C-S	17	20.6784	67.4891	141.263
	18	20.6784	67.4893	141.269
	19	20.6784	67.4894	141.269
	20	20.6784	67.4894	141.269
C-F	18	4.72161	27.7351	77.8219
	19	4.72161	27.7352	77.822
	20	4.72161	27.7352	77.822

Table 4. Frequency parameter Ω for Clamped-Clamped plate

$\varepsilon\downarrow$	$\gamma\downarrow$	mode	g =0	g =1	g =3	g =5
0.1	-0.3	I	31.9442	26.5751	24.7376	23.6827
		II	87.9571	73.1735	68.1141	65.2095
		III	172.63	143.615	133.685	127.984
	-0.1	I	28.8538	24.0041	22.3444	21.3915
		II	79.6206	66.2381	61.6582	59.0289
		III	156.47	130.171	121.17	116.003
	0	I	27.2805	22.6953	21.1261	20.2252
		II	75.3662	62.6989	58.3637	55.8749
		III	148.214	123.302	114.777	109.882
	0.1	I	25.6842	21.3672	19.8898	19.0417
		II	71.0413	59.1008	55.0144	52.6684
		III	139.814	116.314	108.272	103.655
	0.3	I	22.4021	18.6368	17.3482	16.6084
		II	62.1208	51.6797	48.1064	46.055
		III	122.463	101.879	94.8352	90.791
0.2	-0.3	I	41.005	34.113	31.7544	30.4002
		II	113.102	94.092	87.5863	83.8512
		III	221.926	184.625	171.86	164.531
	-0.1	I	36.7603	30.5817	28.4672	27.2532
		II	101.585	84.5112	78.6679	75.3132
		III	199.525	165.989	154.512	147.923
	0	I	34.6093	28.7922	26.8015	25.6585
		II	95.7407	79.6489	74.1418	70.9801
		III	188.149	156.525	145.703	139.489
	0.1	I	32.4343	26.9828	25.1171	24.046
		II	89.8239	74.7265	69.5598	66.5934
		III	176.627	146.94	136.78	130.947
	0.3	I	27.9901	23.2856	21.6756	20.7512
		II	77.7081	64.6471	60.1773	57.6111
		III	153.012	127.294	118.493	113.44
0.3	-0.3	I	54.3459	45.2116	42.0855	40.2908
		II	149.904	124.708	116.086	111.135
		III	294.025	244.606	227.693	217.984
	-0.1	I	48.3654	40.2363	37.4543	35.8571
		II	133.6	111.145	103.46	99.0481
		III	262.229	218.154	203.07	194.411
	0	I	45.3462	37.7245	35.1162	33.6187
		II	125.362	104.292	97.0806	92.9407
		III	246.157	204.784	190.625	182.496
	0.1	I	42.3023	35.1923	32.759	31.362
		II	117.051	97.3774	90.6445	86.7791
		III	229.939	191.291	178.065	170.471
	0.3	I	36.1158	30.0455	27.9681	26.7754
		II	100.137	83.3061	77.5461	74.2392
		III	196.914	163.817	152.49	145.988

Table 5. Frequency parameter Ω for Clamped-Simply Supported plate

ε ↓	γ ↓	mode	g =0	g =1	g =3	g =5
0.1	-0.3	I	20.0179	16.6533	15.5019	14.8408
		II	69.5216	57.8365	53.8376	51.5418
		III	147.127	122.398	113.935	109.077
	-0.1	I	18.5462	15.429	14.3622	13.7498
		II	63.3115	52.6702	49.0285	46.9377
		III	133.724	111.248	103.556	99.14
	0	I	17.7894	14.7994	13.7761	13.1886
		II	60.1441	50.0352	46.5756	44.5895
		III	126.881	105.555	98.2564	94.0664
	0.1	I	17.0151	14.1552	13.1765	12.6146
		II	56.9256	47.3577	44.0832	42.2034
		III	119.921	99.7649	92.8669	88.9067
	0.3	I	15.3994	12.8111	11.9253	11.4168
		II	50.293	41.8399	38.947	37.2861
		III	105.559	87.8166	81.7448	78.2589
0.2	-0.3	I	26.0214	21.6477	20.151	19.2917
		II	89.6712	74.5995	69.4415	66.4803
		III	189.427	157.588	146.692	140.437
	-0.1	I	23.8309	19.8254	18.4547	17.6677
		II	80.9615	67.3536	62.6967	60.023
		III	170.719	142.025	132.205	126.568
	0	I	22.7144	18.8966	17.5901	16.84
		II	76.5436	63.6783	59.2755	56.7477
		III	161.224	134.126	124.852	119.528
	0.1	I	21.5802	17.9531	16.7118	15.9991
		II	72.0733	59.9594	55.8137	53.4335
		III	151.611	126.128	117.407	112.401
	0.3	I	19.242	16.0078	14.901	14.2656
		II	62.9277	52.3509	48.7313	46.6532
		III	131.923	109.75	102.161	97.8048
0.3	-0.3	I	34.9294	29.0586	27.0494	25.8959
		II	119.221	99.1829	92.3252	88.388
		III	251.333	209.09	194.633	186.333
	-0.1	I	31.6425	26.3241	24.504	23.459
		II	106.731	88.7919	82.6526	79.128
		III	224.625	186.87	173.95	166.532
	0	I	29.9777	24.9391	23.2148	22.2248
		II	100.423	83.544	77.7676	74.4513
		III	211.129	175.643	163.499	156.527
	0.1	I	28.2948	23.5391	21.9115	20.9771
		II	94.0612	78.2516	72.8411	69.7349
		III	197.515	164.317	152.956	146.433
	0.3	I	24.8562	20.6784	19.2487	18.4278
		II	81.1247	67.4894	62.8231	60.144
		III	169.81	141.269	131.501	125.894

Table 6. Frequency parameter Ω for Clamped-Free plate

ε ↓	γ ↓	mode	g =0	g =1	g =3	g =5
0.1	-0.3	I	4.481	3.7278	3.47	3.3221
		II	28.1917	23.4533	21.8317	20.9007
		III	84.8977	70.6283	65.7449	62.9413
	-0.1	I	4.3138	3.5888	3.3406	3.1982
		II	26.2505	21.8384	20.3284	19.4616
		III	77.6118	64.567	60.1027	57.5397
	0	I	4.2373	3.5251	3.2814	3.1415
		II	25.2618	21.0159	19.5628	18.7286
		III	73.9006	61.4796	57.2288	54.7883
	0.1	I	4.1671	3.4667	3.2270	3.0894
		II	24.2588	20.1814	18.786	17.9849
		III	70.1342	58.3462	54.312	51.996
	0.3	I	4.0521	3.3711	3.1380	3.00421
		II	22.2003	18.4689	17.192	16.4588
		III	62.3938	51.9068	48.3178	46.2574
0.2	-0.3	I	5.5666	4.631	4.3108	4.127
		II	36.684	30.5182	28.4081	27.1967
		III	109.625	91.1995	84.8937	81.2735
	-0.1	I	5.3046	4.413	4.1078	3.9327
		II	33.7681	28.0925	26.1501	25.0349
		III	99.3106	82.6187	76.9063	73.6267
	0	I	5.181	4.3102	4.0122	3.8411
		II	32.2912	26.8638	25.0064	23.94
		III	94.0845	78.271	72.8591	69.7521
	0.1	I	5.0641	4.2129	3.9216	3.7544
		II	30.799	25.6224	23.8508	22.8337
		III	88.8014	73.8759	68.768	65.8354
	0.3	I	4.8572	4.0408	3.7614	3.6010
		II	27.7576	23.0922	21.4955	20.5789
		III	78.0168	64.9039	60.4163	57.8399
0.3	-0.3	I	7.286	6.0614	5.6423	5.4017
		II	49.2641	40.9839	38.1502	36.5233
		III	145.899	121.376	112.984	108.166
	-0.1	I	6.8639	5.7102	5.3154	5.0887
		II	44.8439	37.3066	34.7272	33.2463
		III	130.99	108.973	101.439	97.1128
	0	I	6.6603	5.5409	5.1578	4.9378
		II	42.6142	35.4517	33.0005	31.5932
		III	123.466	102.714	95.6123	91.535
	0.1	I	6.4634	5.377	5.0052	4.7918
		II	40.3684	33.5833	31.2613	29.9282
		III	115.885	96.4069	89.7412	85.9142
	0.3	I	6.0971	5.0723	4.7216	4.5202
		II	35.815	29.7953	27.7352	26.5524
		III	100.493	83.6024	77.822	74.5033

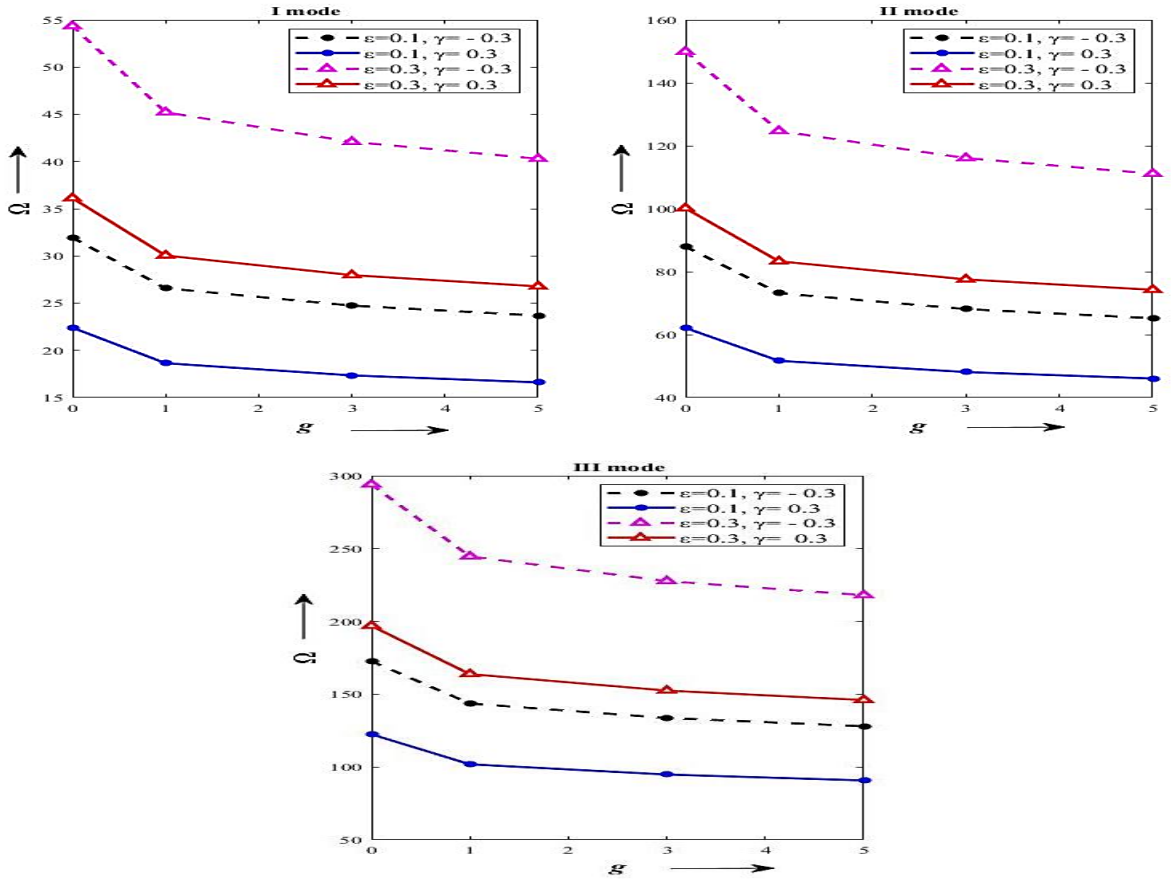

Fig. 2. Frequency parameter Ω versus VFI g for Clamped-Clamped plate

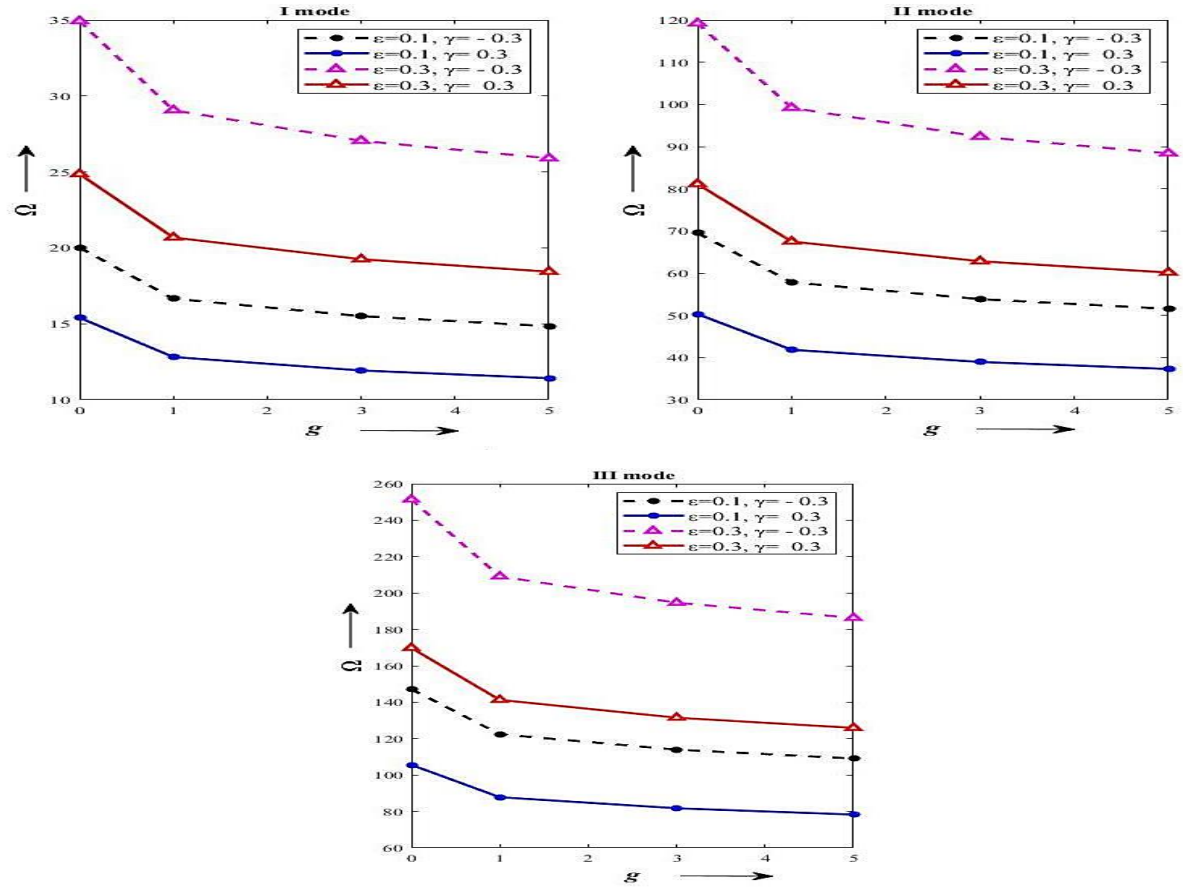

Fig. 3. Frequency parameter Ω versus VFI g for Clamped-Simply Supported plate

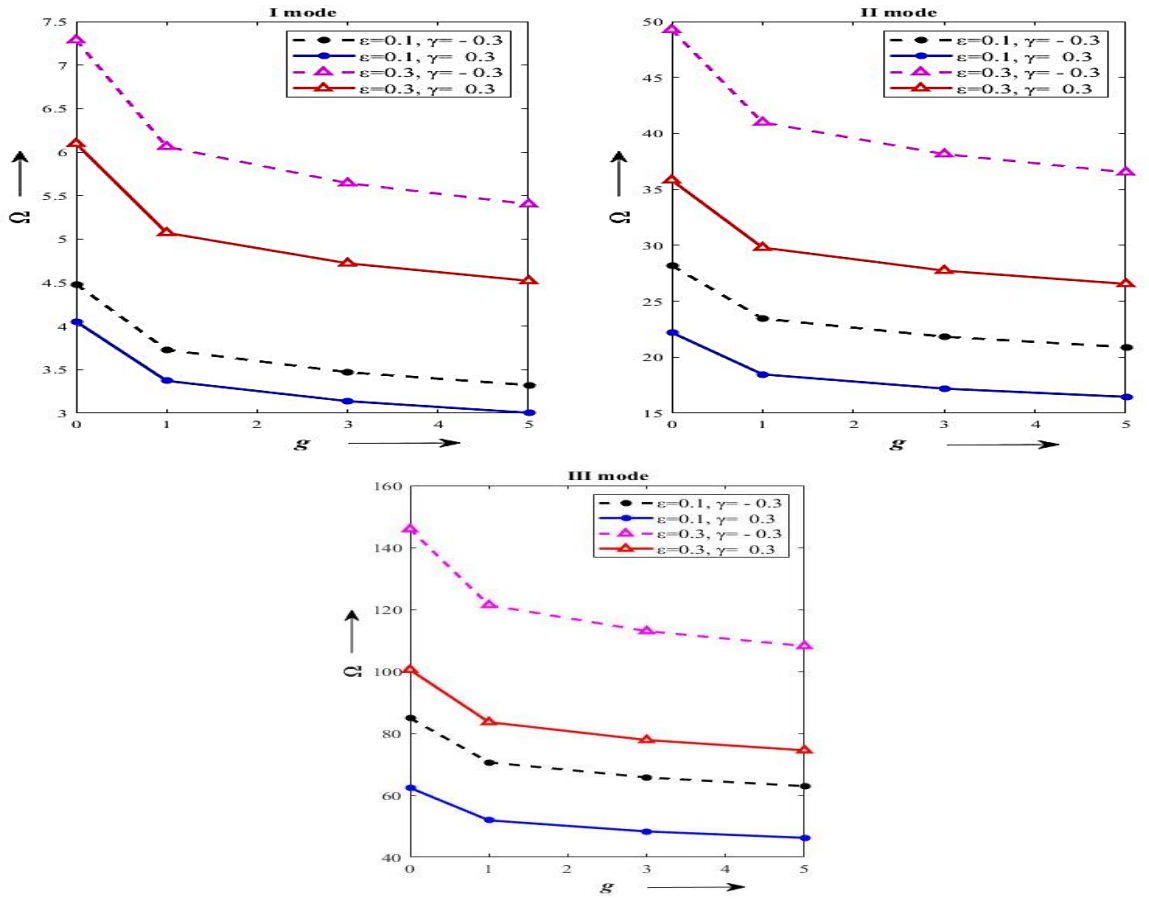

Fig. 4. Frequency parameter Ω versus VFI g for Clamped-Free plate

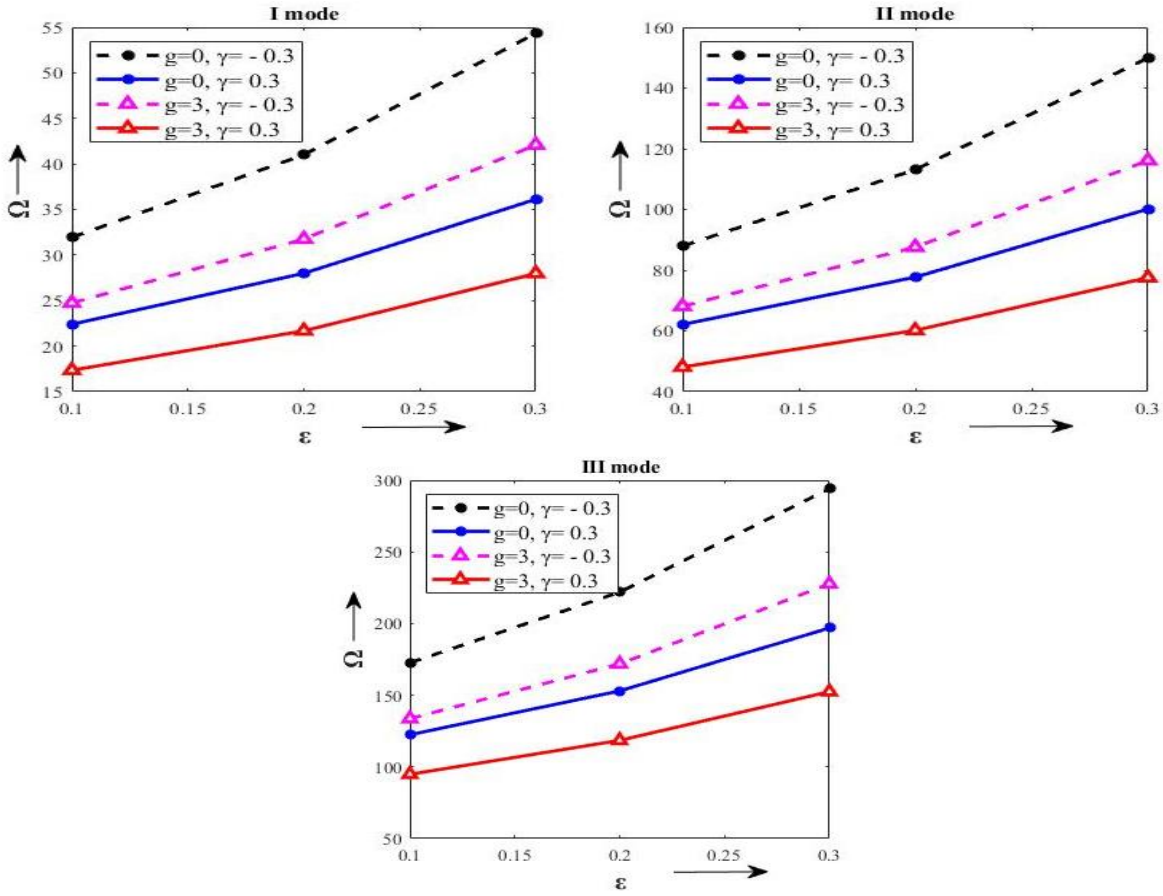

Fig. 5. Frequency parameter Ω versus radii ratio ε for Clamped-Clamped plate

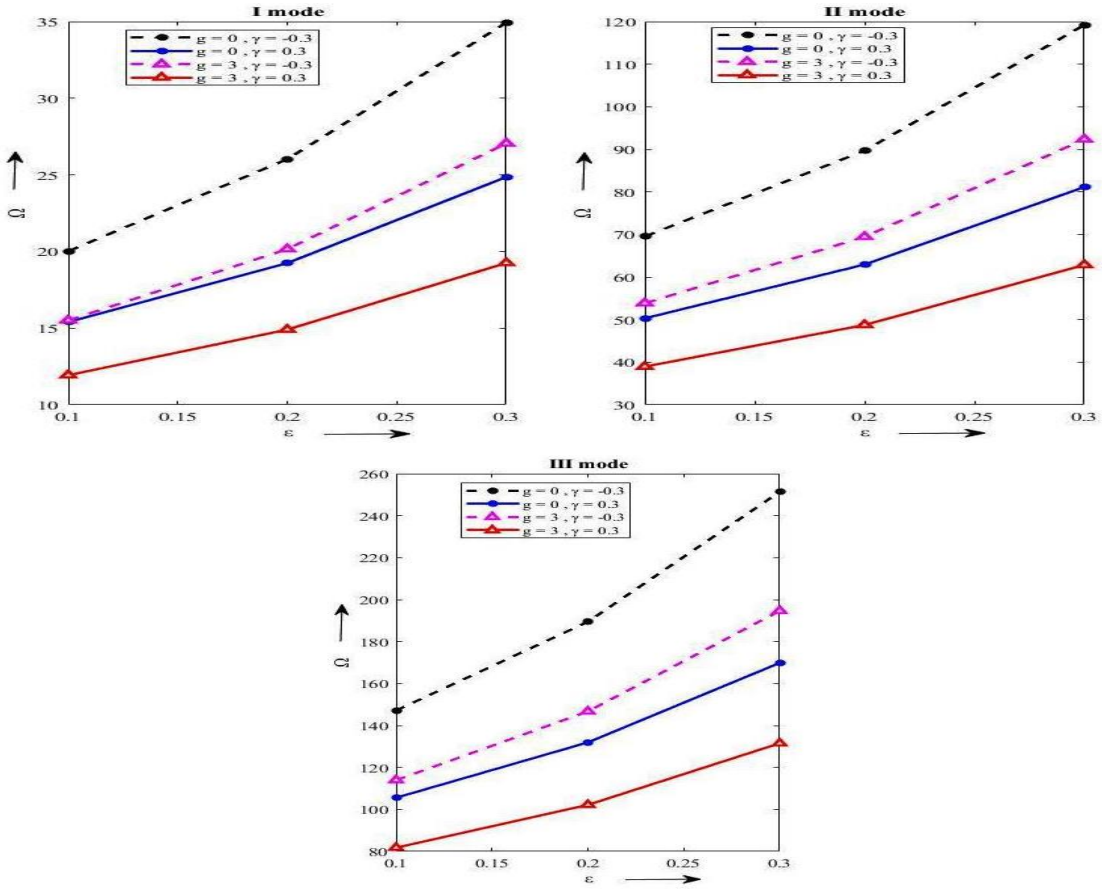

Fig. 6. Frequency parameter Ω versus radii ratio ε for Clamped-Simply Supported plate

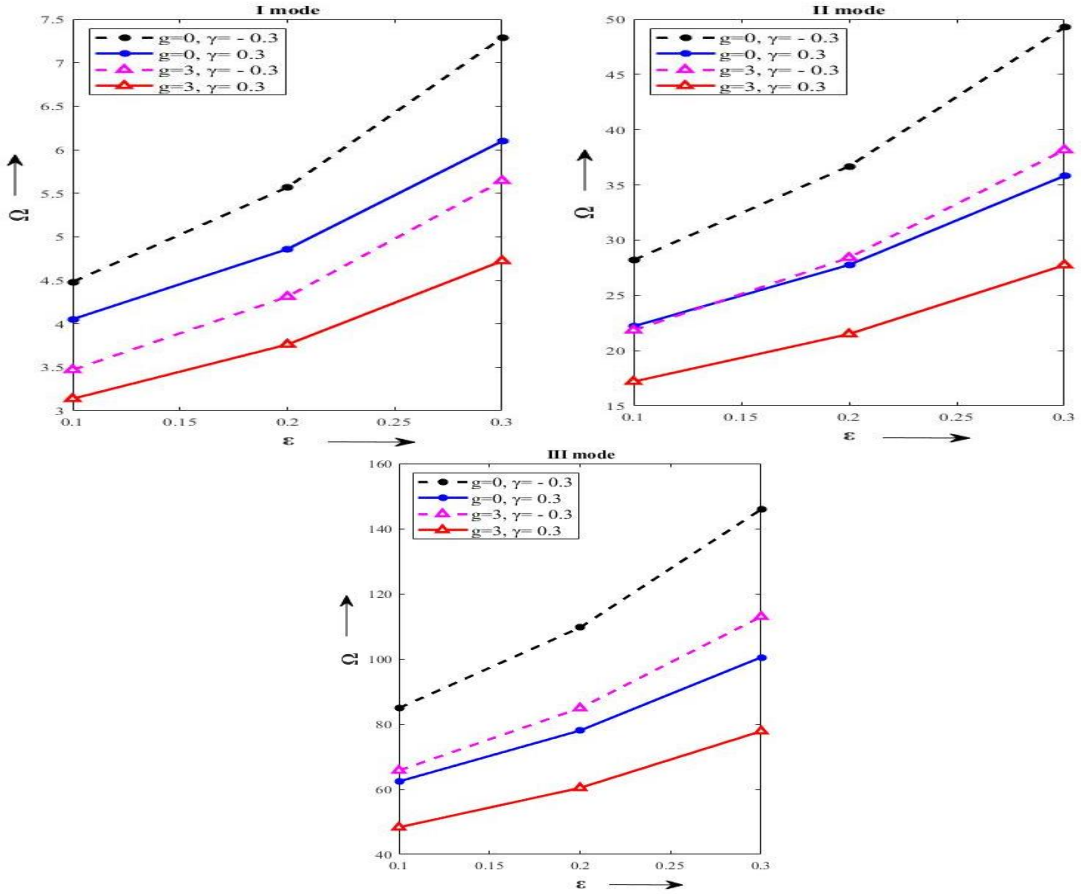

Fig. 7. Frequency parameter Ω versus radii ratio ε for Clamped-Free plate

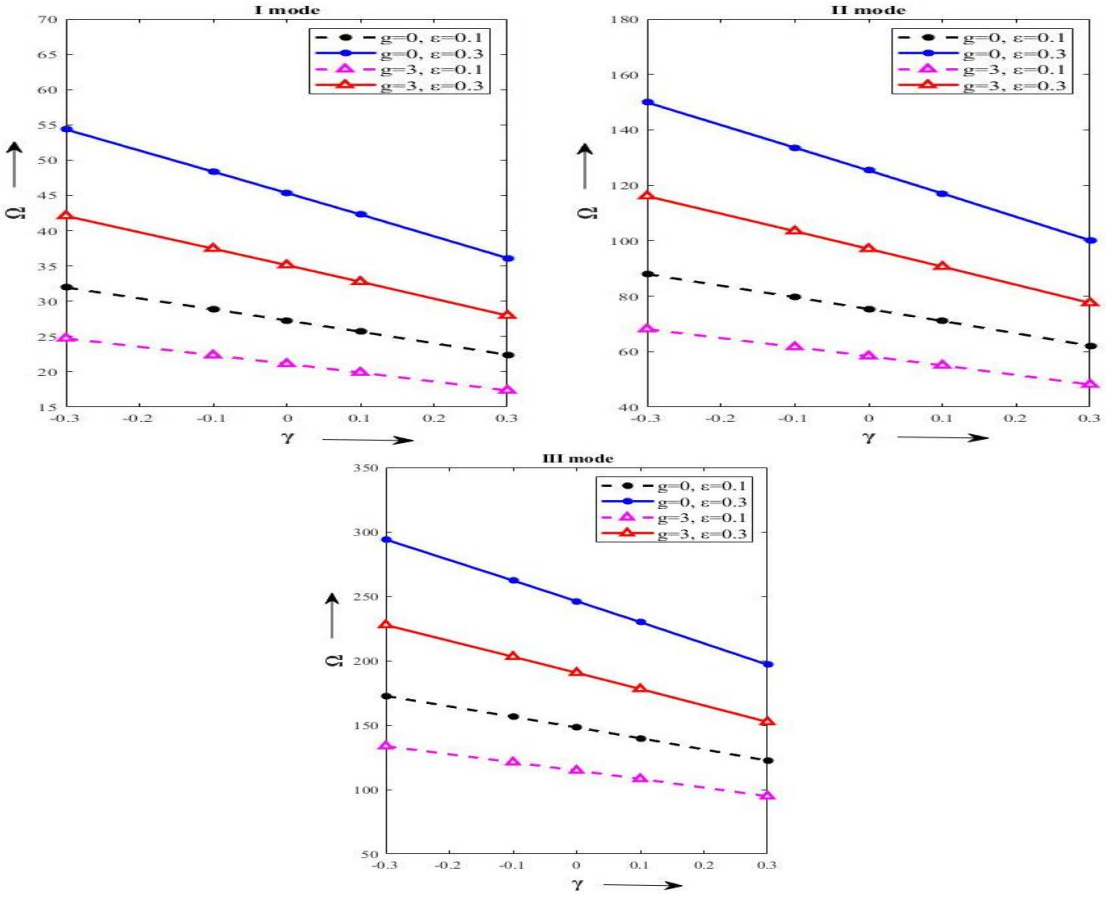

Fig. 8. Frequency parameter Ω versus taper parameter γ for Clamped-Clamped plate

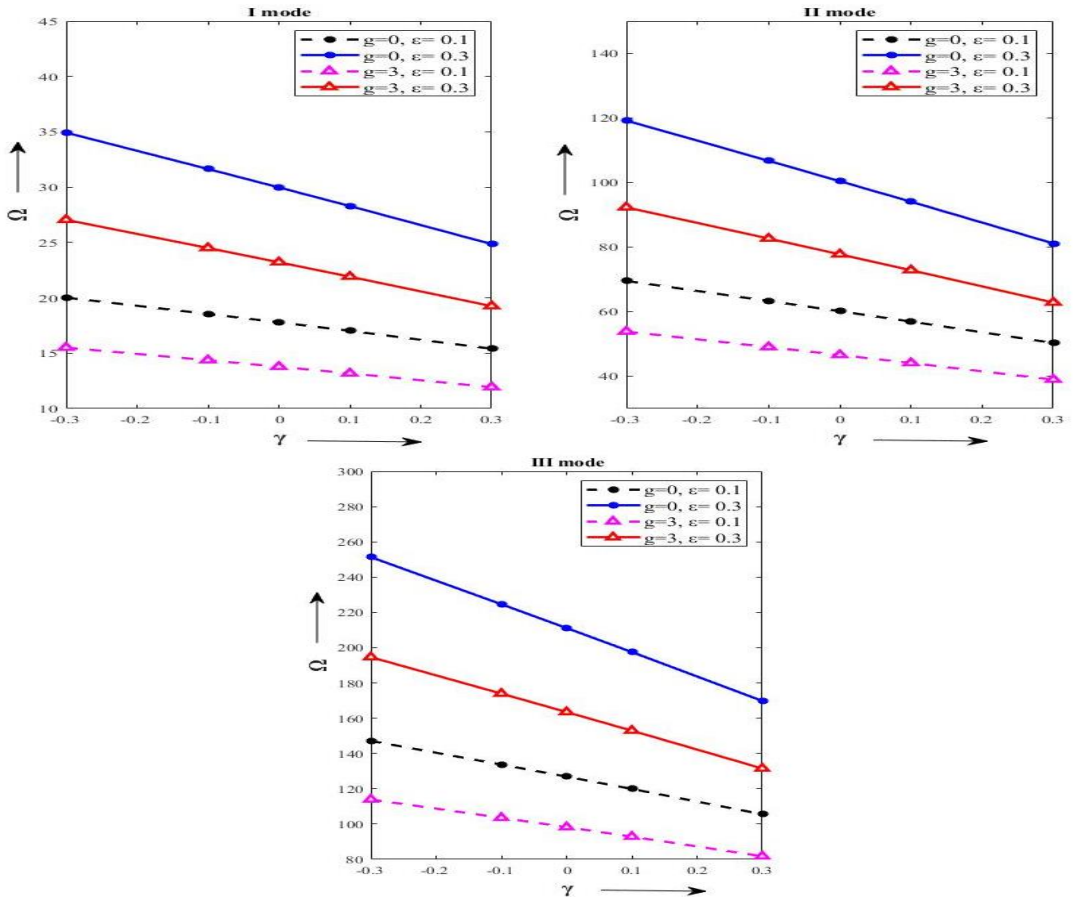

Fig. 9. Frequency parameter Ω versus taper parameter γ for Clamped-Simply Supported plate

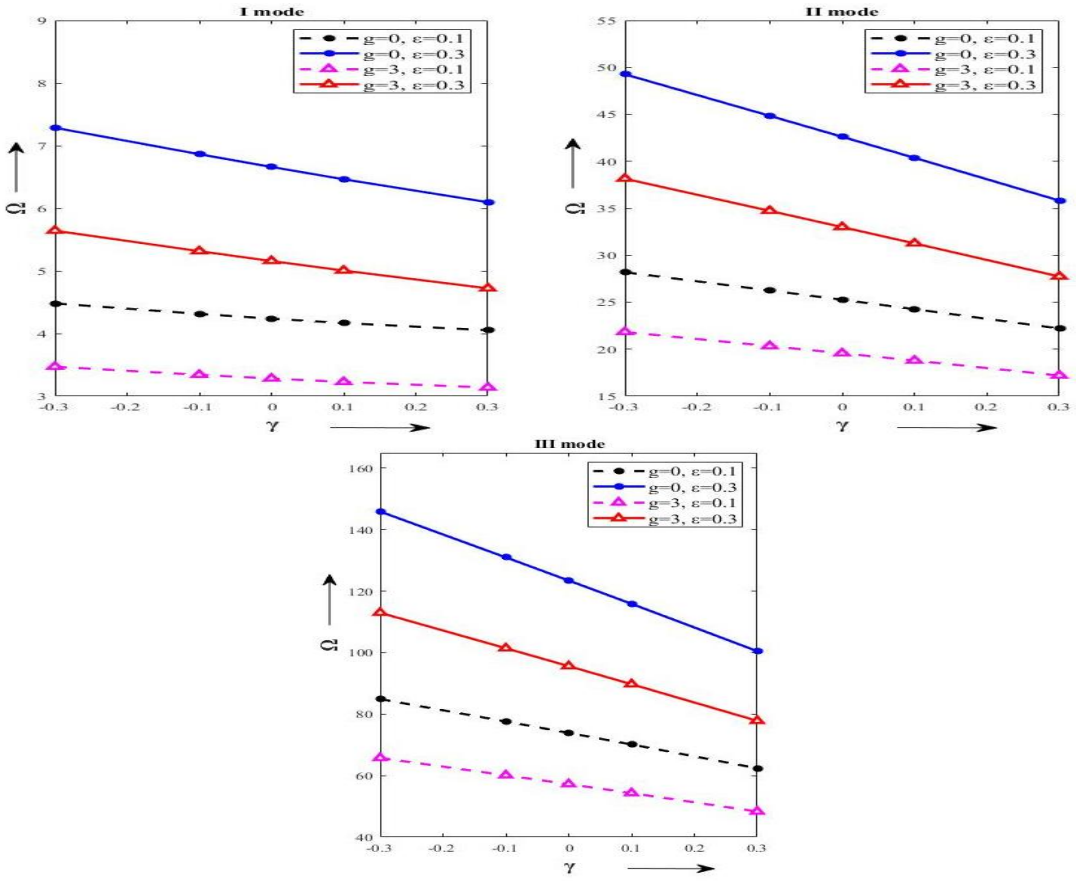

Fig. 10. Frequency parameter Ω versus taper parameter γ for Clamped-Free plate

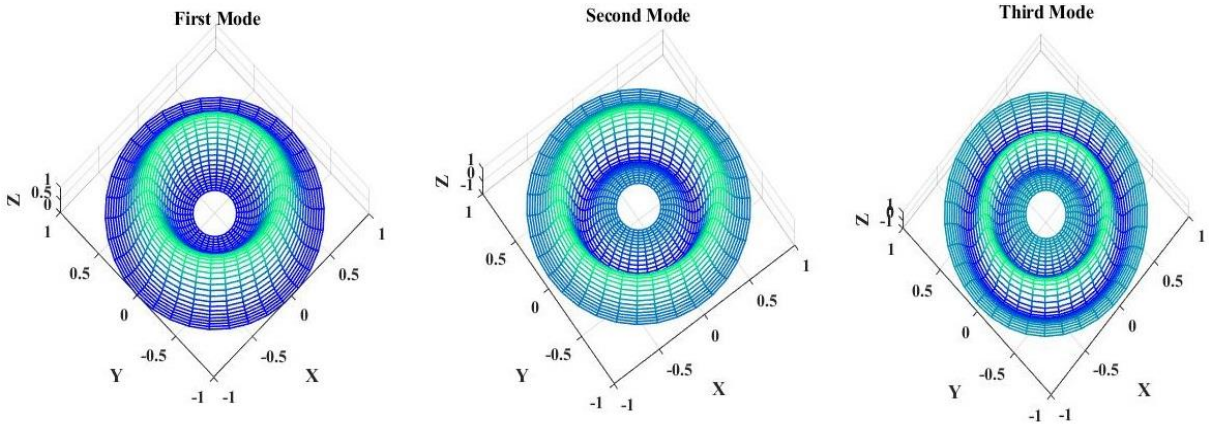

Fig. 11. Three-dimensional mode shapes for Clamped-Clamped plate

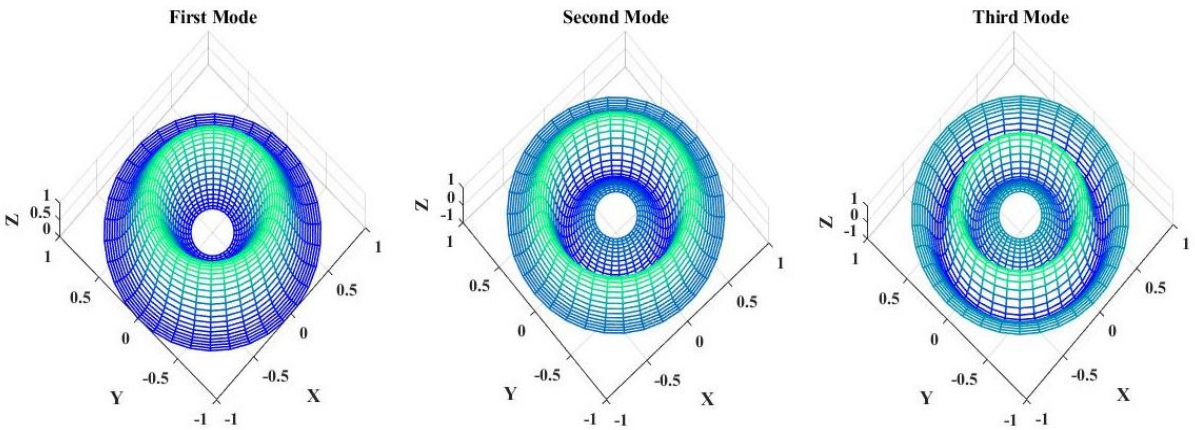

Fig. 12. Three-dimensional mode shapes for Clamped-Simply Supported plate

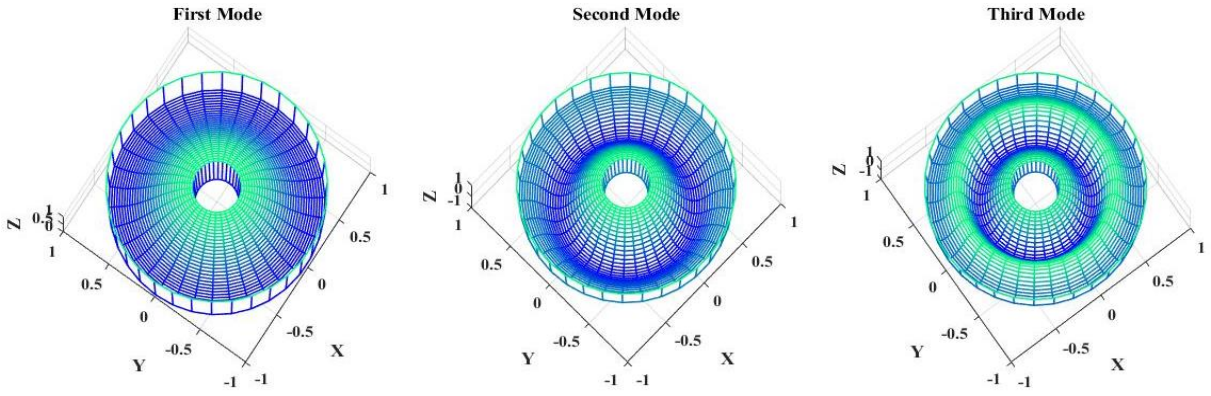

Fig. 13. Three-dimensional mode shapes for Clamped-Free plate

7. Conclusions

In the present article, the effects of linearly varying thickness, VFI, and radius ratio have been examined on the axisymmetric vibrations of annular FGM plates for all three boundary conditions using DTM. The obtained results have been verified with the results found in the literature and also analysed by graphs.

From the tabular and graphical data, the following conclusions have been observed:

1. The decrement in the variation of the constraints, which is applied only on the outer boundary of the plate by fixing the inner boundary as clamped, is the frequency parameter Ω shows a decrease in the following order $\Omega_{CC} > \Omega_{CS} > \Omega_{CF}$.
2. In order to get less impact of vibrations on the structural components, the contribution of the metallic constituent to the ceramic one is more valuable than a fully ceramic plate because the frequency parameter shows less impact on the structure for a composite (i.e., FGM plate taking VFI $g > 0$) than an isotropic (i.e., fully ceramic plate taking VFI $g = 0$).
3. The increasing pattern in the values of the frequency parameter can be seen as the annulus region of the plate increases, i.e., as the value of the radius ratio increases.
4. The decreasing pattern in the values of the frequency parameter has been observed when the plate becomes thicker (i.e., taper parameter γ changes from negative to positive).

Nomenclature

GDQM	Generalized Differential Quadrature Method
FSDT	First Order Shear Deformation Plate Theory
VFI	Volume Fraction Index
DTM	Differential Transform Method
FGM	Functionally Graded Material

Funding Statement

This research did not receive any specific grant from funding agencies in the public, commercial, or not-for-profit sectors.

Conflicts of Interest

The author declares that there is no conflict of interest regarding the publication of this article.

References

[1] Kermani, I.D., Ghayour, M. and Mirdamadi, H.R., 2012. Free vibration analysis of multidirectional functionally graded circular and annular plates. *Journal of Mechanical science and Technology*, 26(11), pp.3399-3410. DOI: 10.1007/s12206-012-0860-2.

[2] Asemi, K., Salehi, M. and Akhlaghi, M., 2014. Three dimensional biaxial buckling analysis of functionally graded annular sector plate fully or partially supported on Winkler elastic foundation. *Aerospace Science and Technology*, 39, pp.426-441. HYPERLINK https://doi.org/10.1016/j.ast.2014.04.011. DOI: 10.1016/j.ast.2014.04.011.

[3] Asemi, K., Salehi, M. and Akhlaghi, M., 2015. Three dimensional graded finite element elasticity shear buckling analysis of FGM annular sector plates. *Aerospace Science and Technology*, 43, pp. 1-13. DOI: 10.1016/j.ast.2015.02.009.

[4] Wang, Q., Shi, D., Liang, Q. and Shi, X., 2016. A unified solution for vibration analysis of functionally graded circular, annular and sector plates with general boundary conditions. *Composites Part B: Engineering*, 88, pp.264-294. HYPERLINK https://doi.org/10.1016/j.compositesb.2015.10.043 DOI: 10.1016/j.compositesb.2015.10.043.

[5] Lal, R. and Ahlawat, N., 2017. Buckling and vibrations of two-directional functionally graded circular plates subjected to

hydrostatic in-plane force. *Journal of Vibration and Control*, 23(13), pp.2111-2127. doi:10.1177/1077546315611328.

[6] Żur, K.K., 2018. Free vibration analysis of elastically supported functionally graded annular plates via quasi-Green's function method. *Composites Part B: Engineering*, 144, pp.37-55. DOI: 10.1016/j.compositesb.2018.02.019.

[7] Civalek, Ö. and Baltacıoğlu, A.K., 2018. Vibration of carbon nanotube reinforced composite (CNTRC) annular sector plates by discrete singular convolution method. *Composite Structures*, 203, pp.458-465. DOI: 10.1016/j.compstruct.2018.07.037

[8] Zhang, N., Khan, T., Guo, H., Shi, S., Zhong, W. and Zhang, W., 2019. Functionally graded materials: an overview of stability, buckling, and free vibration analysis. *Advances in Materials Science and Engineering*, 2019(1), p.1354150. HYPERLINK https://doi.org/10.1155/2019/1354150 DOI: 10.1155/2019/1354150.

[9] Wu, C.P. and Yu, L.T., 2019. Free vibration analysis of bi-directional functionally graded annular plates using finite annular prism methods. *Journal of Mechanical Science and Technology*, 33(5), pp.2267-2279. DOI: 10.1007/s12206-019-0428-5.

[10] Tash, F.Y. and Neya, B.N., 2020. An analytical solution for bending of transversely isotropic thick rectangular plates with variable thickness. *Applied Mathematical Modelling*, 77, pp.1582-1602. DOI: 10.1016/j.apm.2019.08.017.

[11] Eshraghi, I. and Dag, S., 2020. Forced vibrations of functionally graded annular and circular plates by domain-boundary element method. *ZAMM-Journal of Applied Mathematics and Mechanics/Zeitschrift für Angewandte Mathematik und Mechanik*, 100(8), p.e201900048. HYPERLINK https://doi.org/10.1002/zamm.201900048 DOI: 10.1002/zamm.201900048.

[12] Hashemi, S. and Jafari, A.A., 2021. An analytical solution for nonlinear vibration analysis of functionally graded rectangular plate in contact with fluid. *Adv. Appl. Math. Mech.*, 13(4), pp.914-941. DOI: 10.4208/aamm.OA-2019-0333.

[13] Javani, M., Kiani, Y. and Eslami, M.R., 2021. Rapid heating vibrations of FGM annular sector plates. *Engineering with Computers*, 37(1), pp.305-322. DOI: 10.1007/s00366-019-00825-x.

[14] Arefi, M., Moghaddam, S.K., Bidgoli, E.M.R., Kiani, M. and Civalek, O., 2021. Analysis of graphene nanoplatelet reinforced cylindrical shell subjected to thermo-mechanical loads. *Composite Structures*, 255, p.112924. HYPERLINK https://doi.org/10.1142/S0219455426501300 DOI: 10.1142/S0219455426501300

[15] Shahsavari, M., Asemi, K., Babaei, M. and Kiarasi, F., 2021. Numerical investigation on thermal post-buckling of annular sector plates made of FGM via 3D finite element method. *Mechanics of Advanced Composite Structures*, 8(2), pp.309-320. DOI: 10.22075/macs.2021.21158.1293.

[16] Kiarasi, F., Babaei, M., Asemi, K., Dimitri, R. and Tornabene, F., 2022. Free vibration analysis of thick annular functionally graded plate integrated with piezo-magneto-electro-elastic layers in a hygrothermal environment. *Applied Sciences*, 12(20), p.10682. HYPERLINK https://doi.org/10.3390/app122010682 DOI: 10.3390/app122010682.

[17] Sobhani, E., Masoodi, A.R., Civalek, O. and Ahmadi-Pari, A.R., 2022. Agglomerated impact of CNT vs. GNP nanofillers on hybridization of polymer matrix for vibration of coupled hemispherical-conical-conical shells. *Aerospace Science and Technology*, 120, p.107257. HYPERLINK https://doi.org/10.1016/j.ast.2021.107257 DOI: 10.1016/j.ast.2021.107257.

[18] Vasara, D., Khare, S., Sharma, H.K. and Kumar, R., 2022. Free vibration analysis of functionally graded porous circular and annular plates using differential quadrature method. *Forces in Mechanics*, 9, p.100126. DOI: 10.1016/j.finmec.2022.100126.

[19] Huang, C.S. and Chung, W.C., 2023. Analytical solution for the three-dimensional vibration of a rectangular functionally graded material plate with two simply supported opposite faces. *International Journal of Structural Stability and Dynamics*, 23(02), p.2350014. DOI: 10.1142/S0219455423500141.

[20] Shariati, M., Shishehsaz, M. and Mosalmani, R., 2023. Stress-driven Approach to Vibrational Analysis of FGM Annular Nano-plate based on First-order Shear Deformation Plate Theory. *Journal of Applied and Computational Mechanics*, 9(3), pp.637-655. HYPERLINK https://doi.org/10.22055/jacm.2022.41125.3704 DOI: 10.22055/JACM.2022.41125.3704.

[21] Khatoonabadi, M., Jafari, M., Kiarasi, F., Hosseini, M., Babaei, M. and Asemi, K., 2023. Shear buckling response of FG porous annular sector plate reinforced by graphene

platelet subjected to different shear loads. *Journal of Computational Applied Mechanics*, 54(1), pp.68-86. DOI: 10.22059/jcamech.2023.352182.784.

[22] Sharma, S.K. and Ahlawat, N., 2024. Free axisymmetric vibrations of functionally graded material annular plates via DTM. *International Journal of Structural Stability and Dynamics*, 24(03), p.2450027. DOI: 10.1142/S0219455424500275.

[23] Bridjesh, P., Geetha, N.K. and Yelamasetti, B., 2024. Numerical investigation on buckling of two-directional porous functionally graded beam using higher order shear deformation theory. *International Journal on Interactive Design and Manufacturing (IJIDeM)*, 18(5), pp.2805-2818. HYPERLINK http://dx.doi.org/10.1007/s12008-023-01332-6 DOI: 10.1007/s12008-023-01332-6.

[24] Lal, R. and Sharma, S., 2004. Axisymmetric vibrations of non-homogeneous polar orthotropic annular plates of variable thickness. *Journal of sound and vibration*, 272(1-2), pp.245-265. DOI: 10.1016/S0022-460X(03)00329-8.

[25] Alipour, M.M., Shariyat, M. and Shaban, M., 2010. A semi-analytical solution for free vibration of variable thickness two-directional-functionally graded plates on elastic foundations. *International Journal of Mechanics and Materials in Design*, 6(4), pp.293-304. DOI: 10.1007/s10999-010-9134-2.

[26] Hosseini-Hashemi, S., Taher, H.R.D. and Akhavan, H., 2010. Vibration analysis of radially FGM sectorial plates of variable thickness on elastic foundations. *Composite Structures*, 92(7), pp.1734-1743. DOI: 10.1016/j.compstruct.2009.12.016.

[27] Lal, R. and Ahlawat, N., 2015. Axisymmetric vibrations and buckling analysis of functionally graded circular plates via differential transform method. European *Journal of Mechanics-A/Solids*, 52, pp.85-94. DOI: 10.1016/j.euromechsol.2015.02.004.

[28] Lal, R. and Rani, R., 2016. On the use of differential quadrature method in the study of free axisymmetric vibrations of circular sandwich plates of linearly varying thickness. *Journal of vibration and control*, 22(7), pp.1729-1748. HYPERLINK https://doi.org/10.1177/1077546314544695 DOI: 10.1177/1077546314544.

[29] Gupta, A., Jain, N.K., Salhotra, R. and Joshi, P.V., 2018. Effect of crack location on vibration analysis of partially cracked isotropic and FGM micro-plate with non-uniform thickness: an analytical approach. *International Journal of Mechanical Sciences*, 145, pp.410-429. DOI: 10.1016/j.ijmecsci.2018.07.015.

[30] Lal, R. and Saini, R., 2019. Thermal effect on radially symmetric vibrations of temperature-dependent FGM circular plates with nonlinear thickness variation. *Materials Research Express*, 6(8), p.0865f1. DOI: 10.1088/2053-1591/ab24ee.

[31] Ahlawat, N. and Lal, R., 2020. Effect of Winkler foundation on radially symmetric vibrations of bi-directional FGM non-uniform Mindlin's circular plate subjected to in-plane peripheral loading. *Journal of Solid Mechanics*, 12(2), pp.455-475. DOI: 10.22034/jsm.2019.1873720.1466.

[32] Talebitooti, R., Zarastvand, M. and Rouhani, A.S., 2019. Investigating hyperbolic shear deformation theory on vibroacoustic behavior of the infinite functionally graded thick plate. *Latin American Journal of Solids and Structures*, 16(01), p.e139. DOI: 10.1590/1679-78254883.

[33] Lal, R. and Saini, R., 2020. Vibration analysis of functionally graded circular plates of variable thickness under thermal environment by generalized differential quadrature method. *Journal of Vibration and Control*, 26(1-2), pp.73-87. DOI https://doi.org/10.1177/1077546319876.

[34] Jalali, S.K. and Heshmati, M., 2020. Vibration analysis of tapered circular poroelastic plates with radially graded porosity using pseudo-spectral method. *Mechanics of Materials*, 140, p.103240. DOI: 10.1016/j.mechmat.2019.103240.

[35] Tran, M.T. and Thai, S., 2023. Transient analysis of variable thickness multi-directional functionally graded plates using isogeometric analysis. *Multidiscipline Modeling in Materials and Structures*, 19(4), pp.652-679. DOI: 10.1108/MMMS-12-2022-0283.

[36] Zhong, S., Jin, G., Ye, T., Zhang, J., Xue, Y. and Chen, M., 2020. Isogeometric vibration analysis of multi-directional functionally gradient circular, elliptical and sector plates with variable thickness. *Composite Structures*, 250, p.112470. DOI: 10.1016/j.compstruct.2020.112470.

[37] Hashemi, S. and Jafari, A.A., 2021. An analytical solution for nonlinear vibration analysis of functionally graded rectangular plate in contact with fluid. *Adv. Appl. Math. Mech.*, 13(4), pp.914-941. DOI: 10.4208/aamm.OA-2019-0333.

[38] Kumar, V., Singh, S.J., Saran, V.H. and Harsha, S.P., 2021. Exact solution for free vibration analysis of linearly varying thickness FGM plate using Galerkin-Vlasov's method. *Proceedings of the Institution of Mechanical Engineers, Part L: Journal of Materials: Design and Applications*, 235(4), pp.880-897. DOI: 10.1177/146442072098049.

[39] Minh, P.P., Manh, D.T. and Duc, N.D., 2021. Free vibration of cracked FGM plates with variable thickness resting on elastic foundations. *Thin-Walled Structures,* 161, p.107425. DOI: https://doi.org/10.1016/j.tws.2020.107425.

[40] Zarastvand, M.R., Ghassabi, M. and Talebitooti, R., 2021. A review approach for sound propagation prediction of plate constructions. *Archives of Computational Methods in Engineering*, 28(4), pp.2817-2843. DOI: 10.1007/s11831-020-09482-6.

[41] Zarastvand, M.R., Ghassabi, M. and Talebitooti, R., 2022. Prediction of acoustic wave transmission features of the multilayered plate constructions: A review. *Journal of Sandwich Structures & Materials*, 24(1), pp.218-293. DOI: 10.1177/1099636221993891.

[42] Ghafouri, M., Ghassabi, M., Zarastvand, M.R. and Talebitooti, R., 2022. Sound propagation of three-dimensional sandwich panels: influence of three-dimensional re-entrant auxetic core. *Aiaa Journal*, 60(11), pp.6374-6384. DOI: 10.2514/1.J061219.

[43] Kumar, V., Singh, S.J., Saran, V.H. and Harsha, S.P., 2023. Vibration response analysis of tapered porous FGM plate resting on elastic foundation. *International Journal of Structural Stability and Dynamics*, 23(02), p.2350024. DOI: 10.1142/S0219455423500244.

[44] Saini, R., Saini, R., Kumar, A. and Khadimallah, M.A., 2023. Free axisymmetric vibrations of heated non-uniform Bi-directional FGM Mindlin rings employing quadrature approaches. *Thin-Walled Structures*, 184, p.110482. DOI: https://doi.org/10.1016/j.tws.2022.110482.

[45] Hadji, L., Plevris, V., Madan, R. and Ait Atmane, H., 2024. Multi-directional functionally graded sandwich plates: buckling and free vibration analysis with refined plate models under various boundary conditions. *Computation*, 12(4), p.65. DOI: 10.3390/computation12040065.

[46] Islam, T.F. and Kedar, G.D., 2024. Hygrothermal buckling analysis of thin rectangular FGM plate with variable thickness. *Engineering Computations*, 41(3), pp.710-726. HYPERLINK https://doi.org/10.1108/EC-09-2023-0601 DOI: 10.1108/EC-09-2023-0601.

[47] Ahlawat, N. and Saini, R., 2024. Vibration and buckling analysis of elastically supported bi-directional FGM mindlin circular plates having variable thickness. *Journal of Vibration Engineering & Technologies*, 12(1), pp.513-532. DOI: 10.1007/s42417-023-00856-1.

[48] Mandal, R., Singha, T.D., Bandyopadhyay, T. and Karmakar, A., 2025. Influence of porosity on thermal free vibration of rotating porous sigmoid functionally graded plate with bi-directional thickness variation. *Journal of Vibration Engineering & Technologies*, 13(1), p.109. DOI: 10.1007/s42417-024-01639-y.

[49] Jafari Maryaki, F. and Shaterzadeh, A., 2025. Free vibration analysis of functionally graded porous materials complex shells with variable thickness. *AUT Journal of Mechanical Engineering*, 9(2), pp.99-112. DOI: 10.22060/ajme.2025.23494.6137.

[50] Zhou, J.K., 1986. Differential transformation and its applications for electronic circuits. *Huazhong Science & Technology University Press*, China.

[51] Leissa, A.W., 1969. Scientific and Technical Information Division, National Aeronautics and Space Administration. *Vibration of plates,* 160.

[52] Dong, C.Y., 2008. Three-dimensional free vibration analysis of functionally graded annular plates using the Chebyshev -Ritz method. *Materials & Design*, 29(8), pp.1518-1525. DOI: 10.1016/j.matdes.2008.03.001.

[53] Shariyat, M. and Alipour, M.M., 2014. A novel shear correction factor for stress and modal analyses of annular FGM plates with non-uniform inclined tractions and non-uniform elastic foundations. *International Journal of Mechanical Sciences*, 87, pp.60-71. DOI: 10.1016/j.ijmecsci.2014.05.032.

[54] Sharma, S., Gupta, U.S. and Lal, R., 2010. Effect of Pasternak foundation on axisymmetric vibration of polar orthotropic annular plates of varying thickness. *Journal of Vibration and Acoustics*, 132(4), p.041001. HYPERLINK https://doi.org/10.1115/1.4001495 DOI: 10.1115/1.4001495.

[55] Soni, S.R. and Amba-Rao, C.L., 1975. Axisymmetric vibrations of annular plates of variable thickness. *Journal of Sound and Vibration*, 38(4), pp.465-473. DOI: 10.1016/S0022-460X(75)80134-9.